2

Detecting cAMP-induced Epac activation by fluorescenceresonance energy transfer: Epac as a novel cAMP indicator

Detecting cAMP-induced Epac activation by fluorescence resonance energy transfer: Epac as a novel cAMP indicator

Bas Ponsioen[1,2]*, Jun Zhao[3]*, Jurgen Riedl[3], Fried Zwartkruis[3], Gerard van der Krogt [1], Manuela Zaccolo[4], Wouter H. Moolenaar[2], Johannes L. Bos[3+] & Kees Jalink[1++]

[1] Division of Cell Biology, and [2] Division of Cellular Biochemistry andCentre of Biomedical Genetics, TheNetherlands Cancer Institute, Amsterdam, The Netherlands, [3] Department of Physiological Chemistry and Centre of Biomedical Genetics, UMCU, Utrecht, The Netherlands, and [4] Dulbecco Telethon Institute, Venetian Institute of Molecular Medicine, Padova, Italy

Epac1 is a guanine nucleotide exchange factor for Rap1 that is activated by direct binding of cAMP. In vitro studies suggest that cAMP relieves the interaction between the regulatory and catalytic domains of Epac. Here, we monitor Epac1 activation in vivo by using a CFP–Epac–YFP fusion construct. When expressed in mammalian cells, CFP–Epac–YFP shows significant fluorescence resonance energy transfer (FRET). FRET rapidly decreases in response to the cAMP-raising agents, whereas it fully recovers after addition of cAMP-lowering agonists. Thus, by undergoing a cAMP-induced conformational change, CFP–Epac–YFP serves as a highly sensitive cAMP indicator in vivo. When compared with a protein kinase A (PKA)-based sensor, Epac based cAMP probes show an extended dynamic range and a better signal-to-noise ratio; furthermore, as a single polypeptide, CFP–Epac–YFP does not suffer from the technical problems encountered with multisubunit PKA-based sensors. These properties make Epac-based FRET probes the preferred indicators for monitoring cAMP levels in vivo.

Keywords: Epac; PKA; cAMP; FRET

[1]Division of Cell Biology, and [2]Division of Cellular Biochemistry and Centre of Biomedical Genetics, The Netherlands Cancer Institute, Plesmanlaan 121, 1066CX Amsterdam, The Netherlands
[3]Department of Physiological Chemistry and Centre of Biomedical Genetics, UMCU, Universiteitsweg 100, 3584 CG Utrecht, The Netherlands
[4]Dulbecco Telethon Institute, Venetian Institute of Molecular Medicine, Via Orus 2, 35124, Padva, Padova, Italy

*These authors contributed equally to this work
+Corresponding author. Tel: +31 30 253 8988; Fax: +31 30 253 9035;
E-mail: j.l.bos@med.uu.nl
++Corresponding author. Tel: +31 20 512 1933; Fax: +31 20 512 1944;
E-mail: k.jalink@nki.nl

INTRODUCTION

Cyclic AMP is a common second messenger that activates protein kinase A (PKA), cyclic nucleotide-regulated ion channels and Epac (for exchange proteins directly activated by cAMP). Epacs are guanine nucleotide exchange factors (GEFs) for Rap1 and Rap2 (de Rooij et al, 1998). Rap GTPases cycle between an inactive GDP-bound and an active GTP-bound state, with GEFs mediating the exchange of GDP for GTP. Rap proteins are involved in many biological processes, most notably the regulation of cell adhesion through integrins and cadherins (Bos, 2003). The GEF Epac1 consists of a C-terminal catalytic domain characteristic of exchange factors for Ras family GTPases and an N-terminal regulatory domain. The latter domain contains a cAMP-binding site similar to those of protein kinase A (PKA) and, in addition, a DEP domain that mediates membrane attachment (de Rooij et al, 1998; Rehmann et al, 2003a). In vitro studies have shown that cAMP is absolutely required for the activation of Epac (de Rooij et al, 1998). It has been hypothesized that the regulatory domain of Epac functions as an auto-inhibitory domain, which is relieved from inhibition by cAMP, but direct proof for this notion is lacking. In this model, Epac is folded in an inactive conformation at low cAMP levels, thereby preventing Rap binding due to steric hindrance. cAMP binding unfolds the protein, allowing Rap to bind. This is somewhat analogous to the mechanism of PKA regulation by cAMP; in its inactive conformation, two regulatory subunits are bound to two catalytic subunits. On binding of cAMP, this complex falls apart, resulting in the release of active enzymes. In the present study, we set out to measure Epac

activation in vivo by sandwiching Epac between cyan fluorescent protein (CFP) and yellow fluorescent protein (YFP) and then measure fluorescence resonance energy transfer (FRET) between the two fluorescent moieties. FRET, the radiationless transfer of energy from a fluorescent donor to a suitable acceptor fluorophore, depends on fluorophore orientation and on donor–acceptor distance at a molecular scale. We show that in mammalian cells, CFP–Epac–YFP displays significant energy transfer, which rapidly diminishes following a rise in intracellular cAMP and increases again in response to a fall in cAMP. This indicates that cAMP causes a significant conformational change in vivo and supports the unfolding model for Epac activation. Taking advantage of this property, we characterized CFP–Epac–YFP as a FRET sensor for cAMP and generated cytosolic, catalytically dead mutants. We show that the Epac-based cAMP indicators outperform the previously reported PKA-based cAMP sensor (Adams et al, 1991; Zaccolo et al, 2000; Zaccolo & Pozzan, 2002) in several aspects.

RESULTS AND DISCUSSION

cAMP induces a conformational change in Epac

To monitor cAMP-induced conformational changes in Epac, we generated a construct in which Epac1 was fused amino terminally to CFP and carboxy terminally to YFP, as shown in Fig
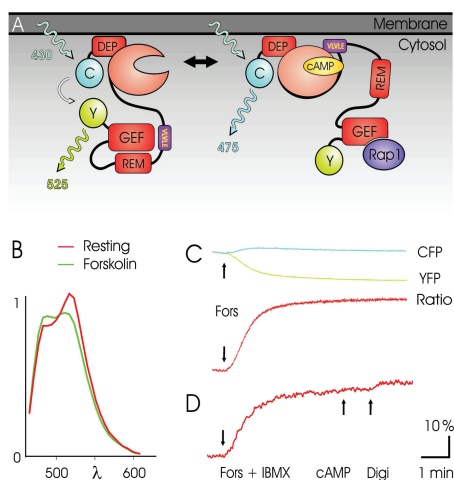
1A. Using a GST–RalGDS assay (supplementary information online), it was confirmed that this construct was able to activate Rap1. CFP–Epac–YFP was transiently expressed in human A431 cells, where it localized to membranes and the cytosol (see below). Fluorescence spectra of these cells revealed significant FRET (Fig 1B, red line), indicating that CFP and YFP are in close proximity (B3–4 nm). Stimulation with forskolin, a direct activator of adenylyl cyclase, significantly decreased FRET (green line). Similar responses were observed in other cell types, including HEK293, N1E-115 and MCF-7 cells. Thus, cAMP induces a significant conformational change in Epac, in support of the unfolding model (Fig 1A). We next analysed the kinetics of cAMP-induced FRET changes by ratiometric recording of CFP and YFP emission using a dualphotometer set-up (see Methods). Within seconds after addition of forskolin, FRET started to decrease, usually dropping to a minimum level in 2–3 min (Fig 1C). In the presence of the phosphodiesterase inhibitor IBMX (100 mM), forskolin evoked an average decrease of 30+3% in CFP/YFP emission ratio. This reflects near-complete saturation of cAMP binding to Epac, as deduced from experiments where cells were subsequently permeabilized with digitonin (10 mg/ml) in the presence of 2mM extracellular cAMP (Fig 1D). This caused at most a moderate (on average, ~3%) further drop in FRET.

Figure 1 | cAMP-induced conformational change in Epac detected by FRET.

(A) Model for the conformational change following binding of cAMP to the regulatory domain of Epac (adapted from Bos, 2003). Following cAMP binding, the VLVLE sequence can interact with the regulatory domain, releasing the inhibition of the GEF domain by the REM domain. FRET between the CFP and YFP tags allows detection of this conformational change. (B) Emission spectra of CFP–Epac–YFP, excited at 430 nm. Red line, resting level; green line, 3 min after forskolin treatment (25 mM). (C) Time course of cAMP-induced CFP–Epac–YFP activation, monitored in A431 cells by FRET. Increases in the ratio CFP/YFP reflect unfolding of Epac. The arrow indicates addition of forskolin (Fors, 25 mM). (D) Cells were treated with forskolin (25 mM) and IBMX (100 mM) and subsequently permeabilized using digitonin (Digi, 10 mg/ml) in the presence of 2mM cAMP.

Epac activation is independent of subcellular localization

CFP–Epac–YFP localized to the cytosol and to membranes, in particular to the nuclear envelope and to perinuclear compartments. We confirmed proper targeting of CFP–Epac–YFP by comparing its distribution with that of immunolabelled endogenous Epac in OVCAR3 cells. Identical localization patterns were observed (Zhao et al, unpublished data), in agreement with a previous report (Qiao et al, 2002). Thus, CFP–Epac–YFP can be used as a FRET probe to image Epac activation. As activation of its downstream target Rap1 is membrane-delimited (Mochizuki et al, 2001; Bivona et al, 2004), we set out to visualize Epac activation throughout the cell by two different imaging FRET techniques (supplementary information online). The results show that, at least in these cells, agonists induce homogeneous FRET changes throughout the cell. Thus, Epac activation is not confined to membranes, indicating that cAMP binding is the main determinant of Epac activation.

CFP–Epac–YFP as a novel fluorescent cAMP indicator

Having shown that FRET changes in CFP–Epac–YFP reflect cAMP binding, we next investigated how well the Epac construct performs as an in vivo sensor for cAMP. We first tested whether CFP–Epac–YFP is insensitive to cGMP, given that cGMP binds to Epac with an affinity similar to that of cAMP, but fails to activate the enzyme (Rehmann et al, 2003b). In N1E-115 neuroblastoma cells, which express soluble guanylyl cyclase, a massive increase in intracellular cGMP levels ensued following stimulation with the NO donor sodium nitroprusside, as recorded by the cGMP-sensitive FRET sensor Cygnet-1 (Honda et al, 2001). In contrast, the Epac FRET signal was not affected by nitroprusside treatment (Fig 2A). We conclude that cGMP does not detectably affect the conformation of Epac. We next tested two cAMP analogues that are specific for either Epac or PKA. As shown in Fig 2B, the Epac-specific compound 8-p-CPT-2'-O-Me-cAMP (Enserink et al, 2002)
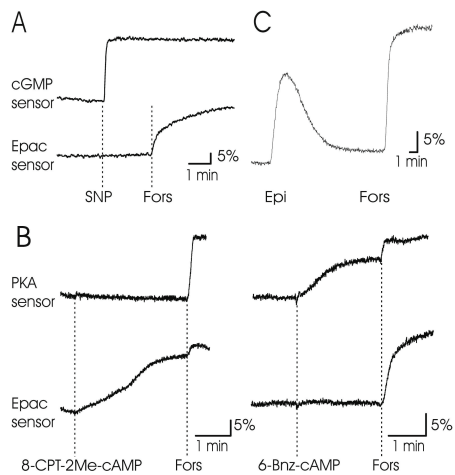

Figure 2 | CFP–Epac–YFP is a specific sensor for cAMP. (A) N1E-115 cells expressing either the cGMP sensor (Cygnet 2.1, upper trace) or the EpaccAMP sensor (lower trace) were treated with sodium nitroprusside (SNP, 1mM) and forskolin (25 mM). The traces depict cAMP- or cGMP-induced loss of FRET as an upward change in CFP/YFP ratio. (B) The PKA- and the Epac-cAMP sensor were tested for their sensitivity to 8-*p*-CPT-2'-OMe- cAMP (8-CPT-2Me-cAMP, 100 mM), a specific activator of Epac, and 6-benzoyl-cAMP (6-Bnz-cAMP, 1mM), which specifically activates PKA. In accordance with biochemical data (not shown), the slow and incomplete increases in CFP/YFP ratio in the upper right and lower left panels are caused by limited diffusion of these compounds over the plasma membrane. (C) Typical example of an agonist-induced cAMP response recorded with CFP–Epac–YFP in a Rat-1 fibroblast. Epi, epinephrine (250nM); forskolin (25 mM) is added to calibrate the response.

reduced FRET in the Epac-cAMP sensor but not in the PKA-cAMP sensor. Conversely, the PKA-specific compound 6-Bnz-cAMP (Christensen et al, 2003) specifically diminished the FRET signal only in cells expressing the PKA-based sensor (Fig 2B). Thus, the Epac-cAMP sensor preserves its specificity for cAMP analogues. We further tested the Epac FRET construct in various cell types, including Rat-1 and NIH3T3 fibroblasts, mouse GE11 epithelial cells, mouse N1E-115 neuroblastoma and human MCF7 breast carcinoma cells. Addition of various cAMP-raising agents and receptor agonists, including forskolin, epinephrine, prostaglandin E1 and neurokinin A, caused robust FRET decreases in all cases. In general, forskolin induced a

sustained decrease in FRET, whereas in most cell types, receptor agonists such as PGE1 and epinephrine (adrenaline) elicited transient signals lasting for 10–15 min (Fig 2C and data not shown). The transient nature of the epinephrine-induced signal is due to homologous receptor desensitization, as a second but distinct stimulus is still capable of decreasing FRET. We conclude that CFP–Epac–YFP is a specific, highly sensitive and reliable indicator of both transient and sustained changes in intracellular cAMP levels.

Inactive, cytosolic mutants have increased FRET responses

To generate a cytosolic variant, we next deleted the DEP domain (amino acids 1–148), which is the main determinant of membrane localization (Qiao et al, 2002; Bos, 2003). Indeed, this chimaera, CFP–Epac(δDEP)–YFP, located almost
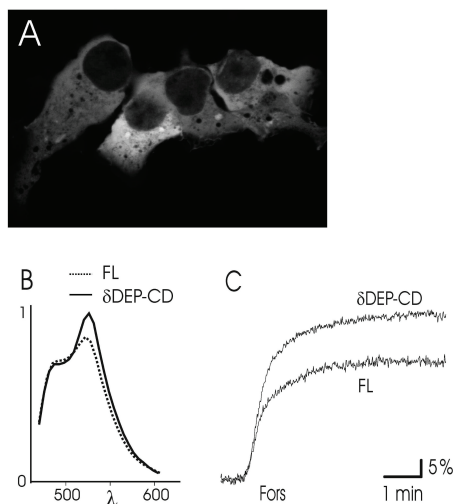

Figure 3 | CFP–Epac(δDEP-CD)–YFP is cytosolic, catalytically inactive and has improved signal-to-noise ratio.
(A) Confocal micrograph of HEK293 cells expressing CFP–Epac(δDEP-CD)–YFP shows absence of membrane labelling. (B) Emission spectra of CFP–Epac–YFP (dashed line) and CFP– Epac(δDEP-CD)–YFP (solid line), excited at 430 nm. (C) Comparison of forskolin-induced change in CFP/YFP ratio in cells expressing CFP– Epac–YFP (FL) and CFP-Epac(δDEP-CD)–YFP. Representative traces from seven experiments each

exclusively in the cytosol (Fig 3A) in HEK293 and other cells. This mutation also diminished Epac's ability to activate Rap1 significantly (supplementary information online). We further introduced mutations (T781A, F782A) to render the indicator catalytically dead. These residues were predicted to affect Rap1 binding based on the crystal structure of SOS, a closely related GEF (Boriack-Sjodin et al, 1998). The resulting construct, CFP–Epac(δDEP-CD)–YFP, showed no detectable Rap1 activation (supplementary information online). Spectral analysis revealed that the basal FRET level in the cytosolic variants was significantly above that of the full-length chimaera (Fig 3B). FRET in CFP–Epac(δDEP-CD)–YFP -expressing cells reliably decreased after stimulation with cAMP-raising agonists. Importantly, maximal changes in CFP/YFP ratio outperformed that of the full-length chimaera by about 50% in magnitude (B45 versus B30%), significantly increasing the signal-to-noise ratio (Fig 3C). Because selectivity remained unaltered when compared with CFP–Epac–YFP (not shown), the cytosolic localization, catalytic inactivity and improved signal-to-noise ratio make CFP–Epac(δDEP-CD)–YFP the indicator of choice for monitoring cytosolic cAMP levels.

Epac cAMP sensors display an extended dynamic range

Previously described PKA-based cAMP sensors are tetramers consisting of two catalytic and two regulatory domains. These probes contain four cAMP-binding sites and have submicromolar (B300 nM) affinity in vivo (Bacskai et al, 1993). cAMP binding in PKA shows cooperativity with an apparent Hill coefficient of 1.6 (Houge et al, 1990). As a consequence, this probe has a steep dose–response relationship that rapidly reaches saturation. In contrast, in vitro studies have shown that the affinity of the single cAMP-binding site in Epac is at least an order of magnitude lower (de Rooij et al, 2000). We determined the affinities of the different fluorescent Epac constructs for cAMP in vitro by fluorescence ratiometry (supplementary information online). The results

showed affinities of B50, B35 and B14 mM for CFP–Epac–YFP, CFP–Epac(δDEP)–YFP and CFP–Epac(δDEP-CD)–YFP, respectively. Thus, the Epac-cAMP sensors should display right-shifted and extended dynamic ranges. To test this notion in vivo, cells expressing either CFP–Epac–YFP or the PKA-cAMP sensor were cocultured on coverslips, and neighbouring cells expressing comparable amounts of Epac and PKA, respectively, were analysed for FRET changes. Dosed photorelease of NPE-cAMP, a membrane-permeable caged cAMP analogue, was used to evoke identical incremental changes in intracellular cAMP in the two neighbouring cells (Fig 4A). Sequential increases in cAMP caused a
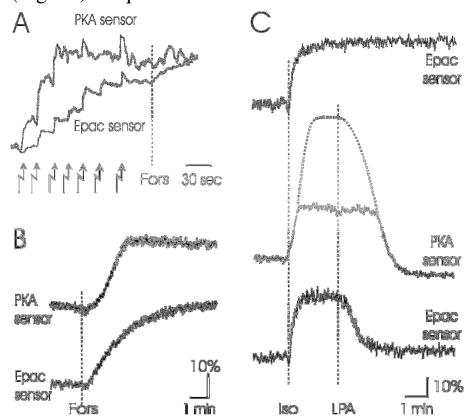

Figure4| The Epac-cAMP sensor exhibits an extended dynamic range as compared with the PKA-cAMP sensor.
(A) Flash photolysis (thin arrows, 1/15 s; thick arrows, 1/4 s) of NPE-caged cAMP in neighbouring A431 cells expressing either PKA-cAMP or Epac-cAMP sensor (as recognized by partial decoration of membranes). Forskolin (50 mM) was added to further increase cAMP levels. Traces are normalized for comparison. (B) Typical responses to forskolin (50 mM), recorded with the PKA- and the EpaccAMP sensor in A431 cells. Response rise times (10–90%) differed significantly (3475 s for PKA, n¼49; 248738 s for Epac, n¼49; Po0.005). Note the sharp transition from the dynamic response range to the saturated plateau phase in the PKA sensor trace. (C) Upper trace: sustained cAMP elevation evoked by isoproterenol (isoprenaline; 10 mM) in a GE11 epithelial cell. Middle and lower traces: registration of cAMP decreases induced by subsequent addition of LPA (5 mM), visualized with the PKA probe and the Epac probe, respectively. Note that Epac reveals the immediate LPA effect, whereas it is obscured by saturation of the PKA-cAMP sensor.

rapid decrease in FRET and subsequent apparent saturation of the response in the PKA sensor, whereas the Epac sensor showed a much larger dynamic range. In line with these observations, the responses to forskolin-induced robust cAMP increases (Fig 4B) were rapid and saturating for the PKA-based sensor, whereas FRET in the Epac-based sensor changed more gradually and often did not saturate completely (Fig 1D). The shifted and extended dynamic range of Epac for cAMP has important consequences for measuring physiological cAMP levels. As shown in Fig 4C, in GE11 cells, isoproterenol (isoprenaline) triggers a rapid and rather sustained FRET change (B30%). In isoproterenol-pretreated cells, addition of lysophosphatidic acid (LPA) resulted in a rapid recovery of the FRET signal, as one would expect for a Gi-coupled receptor agonist that lowers cAMP levels (van Corven et al, 1989). It is to be noted that the PKA-based sensor failed to record this rapid effect of LPA, apparently due to saturation of the probe, but rather reported a substantial lag period (up to several minutes; Fig 4C, middle trace). That it fails to record the true kinetics of the LPA-induced cAMP response becomes evident when the Epac-based sensor is used. As shown in Fig 4C, CFP–Epac–YFP detects the initial fall in cAMP levels within seconds after LPA addition.

CONCLUSIONS

Our results support a model in which cAMP binding to the regulatory domain of Epac releases an inhibitory conformation that prevents binding to Rap1 (de Rooij et al, 2000). Importantly, the FRET signal not only reflects binding of cAMP but also activation of Epac because cGMP, which binds with a similar affinity but fails to activate Epac (Rehmann et al, 2003b), is without effect. We used this property to show that the local, membrane-delimited activation of Rap1 (Mochizuki et al, 2001; Bivona et al, 2004) is not due to local activation of Epac. The uniform Epac activation here observed contrasts with the findings of Zaccolo & Pozzan (2002), who detected subcellular cAMP gradients in cardiac myocytes with the PKA-based cAMP sensor. This

is probably explained by cell-type-specific differences in activity and intracellular distribution of the phosphodiesterases that shape such cAMP gradients, because we failed to detect gradients of cAMP using the PKA probe in our cells. It is to be noted that our in vivo data on the basis of photolysis of NPE-caged cAMP (Fig 4A) strongly support the notion that cAMP differentially regulates its effectors, that is, low cAMP concentrations signal mainly through PKA, whereas at higher doses cAMP exerts additional effects through Epac activation (Zwartkruis et al, 1998). This study further shows that Epac-based FRET constructs are ideally suited as cAMP sensors in that they exhibit improved characteristics compared with the commonly used PKA-based sensors. First, the moderate affinities of our Epac constructs (14–50 mM) result in a right-shifted dose–response relationship that matches physiological cAMP levels (Fig 4). During the review of this manuscript, a K_d of 2.3 mM was reported for a FRET sensor based on Epac's isolated cAMP-binding domain (Nikolaev et al, 2004). Thus, Epac-based sensors provide a wide range of affinities that allows matching the sensors to the anticipated cAMP levels. Second, the PKA regulatory subunits each contain two cAMP-binding sites that exhibit cooperative binding (Hill coefficient of 1.6), resulting in a very steep response. In contrast, the single cAMP-binding domain of Epac1 results in an extended dynamic range. Third, Epac needs only a single cAMP molecule for a 30% FRET change, while four molecules of cAMP are needed to cause a comparable change in two donor–acceptor pairs in PKA. Together with the lower affinity of Epac, this results in reduced buffering of cytosolic cAMP. This is not trivial, as expression levels of cytosolic FRET probes commonly are in the micromolar range (0.1–5 mM; van der Wal et al, 2001), that is, at cAMP levels found in the cytosol following receptor stimulation. Fourth, the Epac-cAMP sensor is a single polypeptide, eliminating expression- and stoichiometry-related problems encountered with the PKA-based versions. For instance, unbalanced expression levels of regulatory and catalytic subunits of PKA hamper

quantitative analyses of FRET changes. Furthermore, a single cDNA construct allows easy generation of stably transfected cell lines, which is often a problem with the PKA-based sensor (unpublished observations). Fifth, monomeric Epac sensors show faster activation kinetics than the slowly dissociating PKA-based sensors (Nikolaev et al, 2004). In addition, the cytosolic CFP–Epac(δDEP-CD)–YFP construct exhibits even larger cAMP-induced FRET changes, resulting in a superior signal-to-noise ratio. Together, these properties make Epac-based FRET probes the preferred fluorescent indicators for monitoring elevated cAMP levels in living cells.

METHODS
Cell culture, transfections and live cell experiments.
Cells were seeded on glass coverslips, cultured and transfected with constructs as described (van Rheenen et al, 2004). Experiments were performed in a culture chamber mounted on an inverted microscope in bicarbonate-buffered saline (containing (in mM) 140 NaCl, 5 KCl, 1 $MgCl_2$, 1 $CaCl_2$, 10 glucose, 23 NaHCO3, with 10mM HEPES added), pH 7.2, kept under 5% CO2, at 37℃ . Agonists and inhibitors were added from concentrated stocks. Expression levels of fluorescent probes were estimated as described (van der Wal et al, 2001).

Dynamic FRET monitoring.
Cells on coverslips were placed on an inverted NIKON microscope and excited at 425 nm. Emission of CFP and YFP was detected simultaneously through 470 ± 20 and 530 ± 25nm band-pass filters. Data were digitized and FRET was expressed as ratio of CFP to YFP signals, the value of which was set to 1.0 at the onset of the experiments. Changes are expressed as per cent deviation from this initial value of 1.0. Loading and flash photolysis of NPE-caged cAMP. Cells were loaded by incubation with 100 mM NPE-caged cAMP for 15 min. Uncaging was with brief pulses of UV light (340–410 nm) from a 100W HBO lamp using a shutter. For comparison, traces were normalized with respect to baseline and final FRET values.

Supplementary information is available at EMBO reports online (http://www.emboreports.org).

REFERENCES

Adams SR, Harootunian AT, Buechler YJ, Taylor SS, Tsien RY (1991) Fluorescence ratio imaging of cyclic AMP in single cells. Nature 349: 694–697

Bacskai BJ, Hochner B, Mahaut-Smith M, Adams SR, Kaang BK, Kandel ER, Tsien RY (1993) Spatially resolved dynamics of cAMP and protein kinase A subunits in Aplysia sensory neurons. Science 260: 222–226

Bivona TG, Wiener HH, Ahearn IM, Silletti J, Chiu VK, Philips MR (2004) Rap1 up-regulation and activation on plasma membrane regulates T cell adhesion. J Cell Biol 164: 461–470

Boriack-Sjodin PA, Margarit SM, Bar-Sagi D, Kuriyan J (1998) The structural basis of the activation of Ras by Sos. Nature 394: 337–343

Bos JL (2003) Epac: a new cAMP target and new avenues in cAMP research. Nat Rev Mol Cell Biol 4: 733–738

Christensen AE et al (2003) cAMP analog mapping of Epac1 and cAMP kinase. Discriminating analogs demonstrate that Epac and cAMP kinase act synergistically to promote PC-12 cell neurite extension. J Biol Chem 278: 35394–35402

de Rooij J, Zwartkruis FJ, Verheijen MH, Cool RH, Nijman SM, Wittinghofer A, Bos JL (1998) Epac is a Rap1 guanine-nucleotide-exchange factor directly activated by cyclic AMP. Nature 396: 474–477

de Rooij J, Rehmann H, van Triest M, Cool RH, Wittinghofer A, Bos JL (2000) Mechanism of regulation of the Epac family of cAMP-dependent RapGEFs. J Biol Chem 275: 20829–20836

Enserink JM, Christensen AE, de Rooij J, van Triest M, Schwede F, Genieser HG, Doskeland SO, Blank JL, Bos JL (2002) A novel Epac-specific cAMP analogue demonstrates independent regulation of Rap1 and ERK. Nat Cell Biol 4: 901–906

Honda A, Adams SR, Sawyer CL, Lev-Ram V, Tsien RY, Dostmann WR (2001) Spatiotemporal dynamics of guanosine 3',5'-cyclic monophosphate revealed by a genetically encoded, fluorescent indicator. Proc Natl Acad Sci USA 98: 2437–2442

Houge G, Steinberg RA, Ogreid D, Doskeland SO (1990) The rate of recombination of the subunits (RI and C) of cAMP-dependent protein kinase depends on whether one or two cAMP molecules are bound per RI monomer. J Biol Chem 265: 19507–19516

Mochizuki N, Yamashita S, Kurokawa K, Ohba Y, Nagai T, Miyawaki A, Matsuda M (2001) Spatio-temporal images of growth-factor-induced activation of Ras and Rap1. Nature 411: 1065–1068

Nikolaev VO, Bunemann M, Hein L, Hannawacker A, Lohse MJ (2004) Novel single chain cAMP sensors for receptor-induced signal propagation. J Biol Chem 279: 37215–37218

Qiao J, Mei FC, Popov VL, Vergara LA, Cheng X (2002) Cell cycle-dependent subcellular localization of exchange factor directly activated by cAMP. J Biol Chem 277: 26581–26586

Rehmann H, Prakash B, Wolf E, Rueppel A, de Rooij J, Bos JL, Wittinghofer A (2003a) Structure and regulation of the cAMP-binding domains of Epac2. Nat Struct Biol 10: 26–32

Rehmann H, Schwede F, Doskeland SO, Wittinghofer A, Bos JL (2003b) Ligand-mediated activation of the cAMP-responsive guanine nucleotide exchange factor Epac. J Biol Chem 278: 38548–38556

van Corven EJ, Groenink A, Jalink K, Eichholtz T, Moolenaar WH (1989) Lysophosphatidate-induced cell proliferation: identification and dissection of signaling pathways mediated by G proteins. Cell 59: 45–54

van der Wal J, Habets R, Varnai P, Balla T, Jalink K (2001) Monitoring agonistinduced phospholipase C activation in live cells by fluorescence resonance energy transfer. J Biol Chem 276: 15337–15344

van Rheenen J, Langeslag M, Jalink K (2004) Correcting confocal acquisition to optimize imaging of fluorescence resonance energy transfer by sensitized emission. Biophys J 86: 2517–2529

Zaccolo M, Pozzan T (2002) Discrete microdomains with high concentration of cAMP in stimulated rat neonatal cardiac myocytes. Science 295: 1711–1715

Zaccolo M, De Giorgi F, Cho CY, Feng L, Knapp T, Negulescu PA, Taylor SS, Tsien RY, Pozzan T (2000) A enetically encoded, fluorescent indicator for cyclic AMP in living cells. Nat Cell Biol 2: 25–29

Zwartkruis FJ, Wolthuis RM, Nabben NM, Franke B, Bos JL (1998) Extracellular signal-regulated activation of Rap1 fails to interfere in Ras effector signalling. EMBO J 17: 5905–5912

Supplementary information

Ponsioen *et al.,* Detecting cAMP-induced Epac activation by fluorescence resonance energy transfer: Epac as a novel cAMP indicator

Methods

Materials. Isoproterenol, 1-oleoyl-LPA, prostaglandin E1, epinephrine and sodium nitroprusside were from Sigma Chemical Co. (St. Louis, MO); IBMX, forskolin, and neurokinin A were from Calbiochem-Novabiochem Corp. (La Jolla, CA); 1-(2-nitrophenyl)ethyl adenosine-3,-5-cyclic monophosphate (NPE-caged cAMP) was from Molecular Probes Inc.Eugene, OR); 8-p-CPT-2-*O*-Me-cAMP and N6-Benzoyladenosine-3,-5-cyclic monophosphate were kindly provided by Hans Gottfried Genieser (Biolog Life Sciences Bremen, Germany).

DNA Constructs. eCFP("non-sticky", A206K (Zacharias *et al.*, 2002), a multiple cloning site with BglII/EcoRV/NheI/SacI restriction sites, and eYFP (A206K) were cloned in-frame, and inserted in pCDNA3 (Invitrogen) using HindIII/XbaI. Full-length Epac1 was generated by PCR using human Epac1 (#AF103905) and cloned in-frame into the restriction sites EcoRV/ NheI of the MCS using the primers 5'-TTGATATCTGATGGTGTTGAGAAGGATGCACC-3' and 5'-GGGGCTAGCTGGCTCCAGCTCTCG GG-3'. The resultant construct contained the linker SGLRSRYL, separating eCFP from Epac1, and ASEL, separating Epac1 from eYFP.

CFP-Epac1(δDEP)-YFP was generated using the upstream primer 5'-TTGATATCAGCC CGTGGGAACTCATG-3' instead, deleting aa 1-148. The latter construct was rendered catalytically dead (CFP-Epac1(δDEP-CD)-YFP) by pointmutating T781A and F782A in the GEF domain.The chosen residues were predicted to affect Rap1-binding based on the crystal structure of the Son of Sevenless (SOS) protein, a GEF for H-Ras and a close family member of Epac (Boriack-Sjodin *et al.*, 1998).

The PKA-based cAMP sensor, consisting of two expression vectors encoding the YFP-tagged catalytic and CFP-tagged regulatory domain of PKA, was as published (Zaccolo *et al.*, 2002; Zaccolo and Pozzan, 2002). The FRET-sensor for cGMP, termed Cygnet-2.1 for *cy*clic *G*MP i*n*dicator using *e*nergy *t*ransfer, consists of a truncated form of the cGMP-dependent protein kinase sandwiched between CFP and YFP and was used as published (Honda *et al.*, 2001).

Fluorescence Lifetime Imaging. FLIM experiments were performed on a Leica inverted DMIRE2 microscope equipped with Lambert Instruments (Leutingewolde, the Netherlands) frequency domain lifetime attachment, controlled by the vendors EZflim software. CFP was excited with ~4 mW of 430 nm light from a LED modulated at 40 MHz and emission was collected at 450-490 nm using an intensified CCD camera. Calculated CFP lifetimes were referenced to a 1 µM solution of Rhodamine-G6 in medium, set at 4.11 ns lifetime. CFP-Epac-YFP expressing cells were cocultured with reference cells that expressed CFP only.
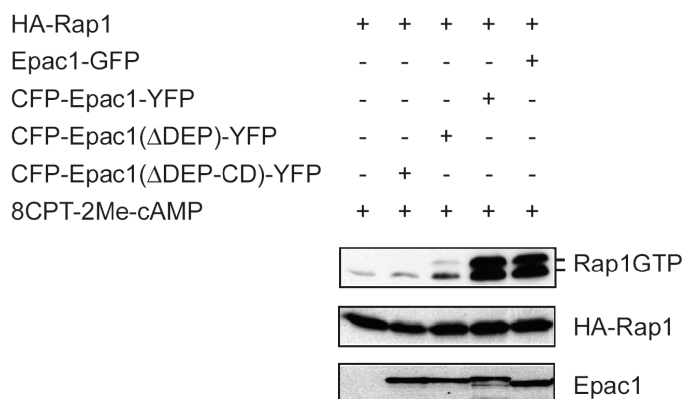
Confocal FRET imaging. We recently described FRET imaging by sensitized emission on a Leica TCS-SP2 confocal microscope (Mannheim, Germany) in detail (van Rheenen *et al.*, 2004). Briefly, reference cells expressing only CFP or YFP were seeded together with the CFP-Epac-YFP expressing cells and simultaneously imaged in the same field of view. Three images were collected: the donor image (CFP, excited at 430 nm and detected from 460-510 nm), sensitized emission image (YFP, excited at 430nm and detected from 528-603 nm) and the acceptor image (YFP, excited at 514 nm and detected from 528-603 nm). All images were shading-corrected. Donor leakthrough in the sensitized emission channel and false acceptor excitation that occurred at 430nm were corrected using correction factors derived from the reference cells as described (van Rheenen *et al.*, 2004). Fret efficiency was expressed by dividing the sensitized emission image with the donor image. Fluorescence spectra were recorded with the λ-scan functionality of the Leica confocal microscope from living cells, excited at 430 nm. Spectra are the mean of 10 scans from different cells.

Supplementary figure 1. *In vivo* **guanine nucleotide exchange (GEF) activity of Epac-based FRET probes**
Different fluorescently tagged Epac constructs were tested for their guanine exchange activity towards Rap1. Indicated constructs were transfected in NIH3T3 cells, which do not express detectable amounts of endogenous Epac1. After 48 hours, cells were stimulated with 100 μM 8-p-CPT-2'-*O*-Me-cAMP for 15 min. Cells were lysed and assayed for GTP-bound Rap1 using GST-RalGDS as an activation-specific probe (de Rooij *et al.*, 1998). **Upper panel**, pull-down samples were probed with an antibody against Rap1 (Santa Cruz, SC-65). The upper band is HA-tagged Rap1, the lower band is endogenous Rap1. **Middle panel**, expression of HA-Rap1 as detected with an anti-HA monoclonal antibody (12CA5). **Lower panel**, expression of Epac1 constructs was verified using an Epac1 specific mouse monoclonal antibody (5D3).
Note that in line with the reported dependence of Epac signaling on correct subcellular localization, loss of the DEP domain significantly interferes with Rap1 activation. Residual activity is completely lost in CFP-Epac(δDEP-CD)-YFP, the mutant that lacks Rap1 binding.

HA-Rap1	+	+	+	+	+
Epac1-GFP	-	-	-	-	+
CFP-Epac1-YFP	-	-	-	+	-
CFP-Epac1(ΔDEP)-YFP	-	-	+	-	-
CFP-Epac1(ΔDEP-CD)-YFP	-	+	-	-	-
8CPT-2Me-cAMP	+	+	+	+	+

Rap1GTP

HA-Rap1

Epac1

Supplementary figure 2. Epac activation is independent of subcellular localization

Activation of the downstream target of Epac1, Rap1, reportedly is membrane-delimited, but conflicting views exist on whether this predominantly occurs at endomembranes or at the plasma membrane (Mochizuki *et al.*, 2001;Bivona *et al.*, 2004). We therefore set out to visualize Epac activation throughout the cell by two different FRET techniques. Initially, we confirmed that tagging of Epac with GFPs does not interfere with its proper localization by comparing the cellular distribution of CFP-Epac-YFP to that of immunolabeled endogenous Epac in OVCAR3 cells. In good agreement with published data for untagged Epac (Qiao *et al.*, 2002), CFP-Epac-YFP localized in the cytosol as well as to membranes (the nuclear envelope, perinuclear membranes, and to a lesser extent the plasma membrane). Details will be published elsewhere (Zhao *et al.,* in preparation).
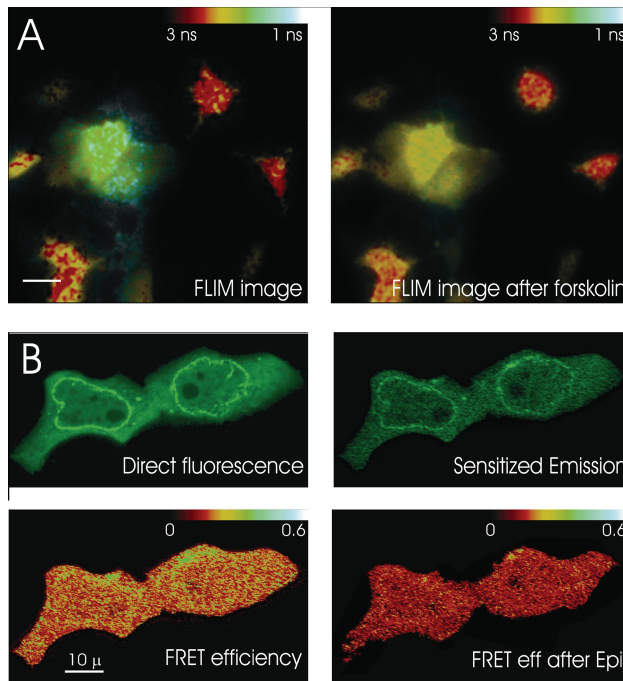
Supplementary Figure 2. Spatial distribution of Epac activity as detected by fluorescence resonance.

A) (left panel) FRET in CFP-Epac-YFP expressing A431 cells as detected by FLIM. The homogeneous lifetime of ~1.7 ns throughout the cell indicates ~30% FRET efficiency. For reference, CFP in control cells displays a lifetime of ~2.4 ns. (right panel) Stimulation with forskolin (1 μM) decreases FRET, causing the lifetime to increase to ~2.2 ns. **B)** Confocal images of an A431 cell expressing CFP-Epac-YFP. Upper left, YFP fluorescence; upper right, sensitized emission, i.e. calculated YFP emission resulting from FRET; lower left, calculated FRET efficiency in resting cell; lower right, FRET efficiency after epinephrine treatment (250 nM).

Widefield Fluorescence Lifetime IMaging (FLIM; see Methods) reports FRET quantitatively as a decrease in the excited-state lifetime of the fluorescent donor molecule. For reference, A431 cells expressing CFP-Epac-YFP were imaged along with HEK293 control cells expressing cytosolic CFP. In resting cells, our FLIM analysis failed to reveal spatial differences in FRET efficiency (Fig. 2A, left panel). Furthermore, activation of Epac with cAMP-raising agonists caused a similar FRET decrease throughout the cells (Fig. 2A, right panel).To better resolve subcellular details, we employed a recently developed, highly corrected confocal laser scanning FRET microscopy approach (van Rheenen *et al.*, 2004) that allows discrimination of CFP-Epac-YFP activation in the cytosol and at membranes. In the cell types studied, Epac activation state as deduced from FRET did not depend on membrane localization (lower left panel). cAMP-raising agonists such as epinephrine (250 nM) caused similar FRET changes at membranes and in the cytosol (lower right panel). The homogeneous FRET values determined for CFP-Epac-YFP throughout the cells are likely due to the rapid diffusion of cAMP in the cytosol. Taken together, our data demonstrate that Epac activation is not localized to membranes and further indicate that binding to cAMP is the main determinant of Epac activation.

Supplementary figure 3. Fluorescently tagged Epac constructs bind cAMP with micromolar affinities
To determine dissociation constants (Kd) towards cAMP, five 15-cm petridishes of HEK293 cells were transfected for each of the constructs. Cells were harvested 24h post transfection, washed in PBS and homogenized in hypotonic medium (PBS:H2O, 1:2) with a Downs piston.The homogenate was cleared by high-speed centrifugation for 10 minutes and subsequently ionic concentrations were corrected towards intracellular levels
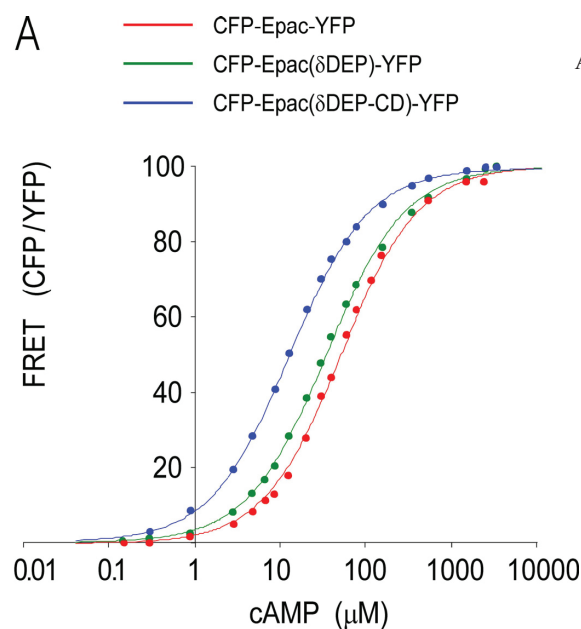
A) Dose-response relationship for cAMP-induced FRET changes for CFP-Epac-YFP (red), CFPEpac(δDEP)-YFP (green), and CFP-Epac(δDEP-CD)-YFP (blue) *in vitro*. Apparent dissociation constants were 50 +/- 3 μM, 35 +/- 3 μM, and 14 +/- 2 μM, respectively (N=3). Hill coefficients did not differ significantly from 1 (0.97, 0.95 and 0.94, respectively). Shown are data and fitted curve of a representative example.

(in mM: 140 KCl, 5 NaCl, 1 MgCl2 and 10 HEPES for pH 7.2). FRET changes caused by consecutive additions of cAMP were recorded in the stirred cuvet of a PTI Quantamaster dual channel spectrofluorimeter (Lawrenceville, NJ). FRET was expressed as the ratio of the YFP channel (530 +/-10 nm) and the CFP channel (490 +/- 10 nm), when excited at 420 +/-3 nm. For analysis, we used the Hillfunction:

$FRET([cAMP]) = FRETmax * ([cAMP]^n / (Kd^n + [cAMP]^n))$.

References

Bivona,T.G., Wiener,H.H., Ahearn,I.M., Silletti,J., Chiu,V.K. and Philips,M.R. (2004) Rap1 upregulation and activation on plasma membrane regulates T cell adhesion. *J Cell Biol*, **164**, 461-470.

Boriack-Sjodin,P.A., Margarit,S.M., Bar-Sagi,D. and Kuriyan,J. (1998) The structural basis of the activation of Ras by Sos. *Nature*, **394**, 337-343.

de Rooij,J., Zwartkruis,F.J., Verheijen,M.H., Cool,R.H., Nijman,S.M., Wittinghofer,A. and Bos,J. L. (1998) Epac is a Rap1 guanine-nucleotide-exchange factor directly activated by cyclic AMP. *Nature*, **396**, 474-477.

Honda,A., Adams,S.R., Sawyer,C.L., Lev-Ram,V., Tsien,R.Y. and Dostmann,W.R. (2001) Spatiotemporal dynamics of guanosine 3',5'-cyclic monophosphate revealed by a genetically encoded, fluorescent indicator. *Proc Natl Acad Sci U S A*, **98**, 2437-2442.

Mochizuki,N., Yamashita,S., Kurokawa,K., Ohba,Y., Nagai,T., Miyawaki,A. and Matsuda,M.(2001) Spatio-temporal images of growth-factor-induced activation of Ras and Rap1. *Nature*, **411**, 1065-1068.

Qiao,J., Mei,F.C., Popov,V.L., Vergara,L.A. and Cheng,X. (2002) Cell cycle-dependent subcellular localization of exchange factor directly activated by cAMP. *J Biol Chem*, **277**, 26581-26586.

van Rheenen,J., Langeslag,M. and Jalink,K. (2004) Correcting confocal acquisition to optimize imaging of fluorescence resonance energy transfer by sensitized emission. *Biophys J*, **86**, 2517-2529.

Zaccolo,M., Magalhaes,P. and Pozzan,T. (2002) Compartmentalisation of cAMP and Ca(2+) signals. *Curr Opin Cell Biol*, **14**, 160-166.

Zaccolo,M. and Pozzan,T. (2002) Discrete microdomains with high concentration of cAMP in stimulated rat neonatal cardiac myocytes. *Science*, **295**, 1711-1715.

Zacharias,D.A., Violin,J.D., Newton,A.C. and Tsien,R.Y. (2002) Partitioning of lipid-modified monomeric GFPs into membrane microdomains of live cells. *Science*, **296**, 913-916.

Subcellular localisation of Epac